AUBE '01

12TH INTERNATIONAL CONFERENCE ON AUTOMATIC FIRE DETECTION

March 25 - 28, 2001
National Institute Of Standards and Technology
Gaithersburg, Maryland U.S.A.

PROCEEDINGS

Editors: Kellie Beall, William Grosshandler and Heinz Luck

NIST
National Institute of Standards and Technology
Technology Administration, U.S. Department of Commerce

Darryl W. Weinert*, Thomas Cleary, and George W. Mulholland

National Institute of Standards and Technology, Gaithersburg, MD, U.S.A.

*Guest Researcher on leave from the Center for Environmental Safety and Risk Engineering, Victoria University, Melbourne, PO Box 14428, VIC 8001, AUSTRALIA

Size Distribution and Light Scattering Properties of Test Smokes

1. Introduction

It is well documented that the response of a detector to smoke depends on the detector design and the particular smoke that it is exposed to. Detailed measurements of smoke particle size distributions and optical properties from fires could yield a better understanding of existing detector designs and facilitate design improvements; NIST is making such measurements now on smokes produced in the fire emulator/detector evaluator (FEDE) [1,2]. One flaming (propylene) and two non-flaming tests smokes (cotton smolder and wood pyrolysis) are studied in this paper. The smokes produced by the non-flaming fuels are similar to two of the smokes produced by the EN54 test fires. The work presented here complement previous measurements of test smoke size distributions and various moments of the distributions [3,4], as well as light scattering studies [5,6]. Our results provide the size distribution using a cascade impactor and an optical particle counter. Our light scattering measurements provide the first differential cross sections for these three smokes on a per mass basis. In addition light scattering data for ethylene and acetylene smoke are expressed in terms of the scattering parameter q to assess the generality of the fractal description of such smokes. An approach based on the scattering parameter for discrimination between smoke particles from flaming and non-flaming fires is discussed.

2. Smoke Generation and Sampling

The smokes are generated in the FEDE and extracted for size distribution and light scattering analysis. A detailed description of the FEDE and its operation is presented in another paper at this conference [2]. The flaming test smoke is soot from a propylene

diffusion flame burner attached to the FEDE duct. Due to the high soot yield from propylene diffusion flames, the burner can output a large amount of soot at moderate fuel flow. Smoke concentration in the FE/DE is controlled by varying the burner fuel flow and the amount of smoke directed to the duct. The smoke concentration is constant over the aerosol extraction time. One of the non-flaming fuel smokes, cotton wicks used in EN54 (part **9,** test fire **3)** is generated by a staged-wick-ignition-smolderdevice inside the FE/DE. Wicks are smoldered and smoke was collected when the light extinction measurement indicated a steady smoke concentration in the duct. The wood pyrolysis smoke is generated by heating wood blocks identical to those specified in EN54 (part 9, test fire 2) on an electrically heated hot plate. The rate of smoke evolution from the wood is characterized by a gradually increasing concentration as the wood block heats up followed by a period of quasi-steady-state smoke production.

For size distribution measurements of the smokes two instruments were used; an optical particle counter (OPC) and a cascade impactor. The smoke produced in the FE/DE is sampled directly into a MOUDI cascade impactor **[7]** at **30** L min^{-1} for determining the **mass** distribution, while for the other measurements the smokes were collected in a particle-free drum **(0.24** m^3) by drawing smoke from the test section of the FEDE into the drum. For the OPC about 20 L of smoke was drawn in to the drum at a nominal rate of 10 L min^{-1} and in the case of the scattering cross section, about 120 L of smoke was sampled into the drum at a rate of 20 L min^{-1}. The smoke filled drum was then transported to the laboratory where the light scattering instruments used in the smoke characterization were situated. These instruments were an OPC used to measure the number distribution and the large agglomerate optical facility (LAOF) developed at NIST **[8]** for measuring differential scattering cross sections of smoke particles. During the 10 to **30** minutes for obtaining the light scattering data there was little change in the differential scattering cross section.

3. Size Distribution Measurements

The optical particle counter (OPC) utilizes an active cavity laser scattering cell and focused jet of particles to determine the particle's number size distribution from the

scattered light signal of individual particles. The instrument is calibrated with monodisperse polystyrene spheres to relate the detector output to the particle size. An additional dilution by about a factor of 50 was required to dilute the smoke concentration below the 10^4 particles cm^{-3} operating threshold; above this level there would be more than one particle in the scattering volume causing coincidence errors. The cascade impactor makes use of an airborne particle's inertia to impact large particles in preference to small particles as they pass through the impactor. Each stage of the impactor collects the particles of a given range of aerodynamic diameter, which is the diameter of a sphere of unit density having the same settling velocity as the particle. The impactor stages are covered by aluminum foil which is weighed before being placed on the stage. After the smoke is sampled through the impactor the foils are removed and their weight measured again. The weight of the collected particles is divided by $\Delta \log D$ of the two adjacent 50 % cut points, then plotted against the stages mid-range diameter to give the **mass** distribution as a function of aerodynamic diameter. Figure 1 shows the mass distribution results from the impactor and the calculation of the volume distribution from the number distribution data of the OPC. The large spikes in the OPC volume distribution are a result of changes in the width of the size channel from as small as 0.005 μm for 0.07 μm particles to 0.1 μm width for 0.7 μm particles.

Almost half, **48** %, of the total **mass** of the cotton wick smoke was found to be below the last stage of the impactor, **i.e.** less than *0.056* μm in aerodynamic diameter, implying that the cotton lamp wick smoke is bimodal, The volume distribution OPC data and impactor mass distribution, both shown in Figure 1, agree well for cotton wick smoke for particle sizes larger than 0.07 pm. In the case of the wood smoke, the comparison is incomplete because of the lack of the OPC data above 1 pm. The fact that only **2.2** % of the total wood smoke **mass** was found below *0.056* μm indicates that the **mass** size distribution is unimodal.

The wood smoke examined in these experiments were found to have a mass mean aerodynamic diameter (MMAD) of about **1.6** μm and a geometric standard deviation **(GSD)** of about **2.** If the mode of the distribution of the cotton wick smoke is treated as

a single log-normal distribution then it has a MMAD of about 0.3 μm and a GSD of about 1.9. The GSD values are typical of polydisperse aerosol systems. The cotton wick smoke has a substantially smaller mean aerodynamic diameter compared to the wood smoke when considering the single mode of cotton wick smoke measured. The number

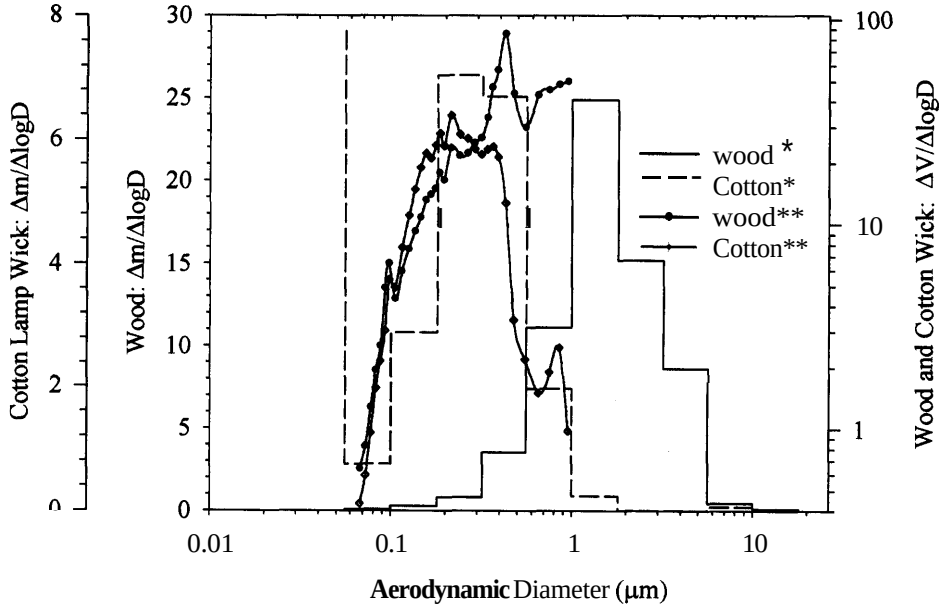

Figure 1: Mass distribution from impactor data (*- outlined bar graph, separate scales on left) and Volume distribution calculated from OPC data (** - line connects data points, scale on right) for non-flaming wood and cotton lamp wick smokes.

distribution from the OPC (not shown) gives a mean number diameter for wood and cotton wick smokes as 0.14 pm. Helsper et al. [3] used a bimodal log-normal distribution to describe the size distribution of smoke from EN 54 test fuels. Our results are close to the median size of the second (i.e. highest) mode of the distribution of [3], 0.14 μm and 0.13 μm for smoldering wood and smoldered cotton wick respectively. Our cascade impactor data is consistent with [3] for the cotton wick as it indicates a second peak below 0.056 μm, but is inconclusive when considering a second peak below 0.056 μm for the wood smoke.

The cotton wick smoke particles less than **0.056** μm will contribute very little to light extinction or light scattering signals; however, these small particles are expected to contribute significantly to an ionization smoke detector signal, which is proportional to the product of the number concentration and mean diameter. This was verified in the FE/DE by measuring the response of a measuring ionisation chamber (MIC) to both smokes along with light extinction measurements [2]. It was found that the ionization response was about **3.4** times greater for cotton wick smoke compared to smoke from pyrolysed wood for the average extinction coefficient over the time of smoke collection.

In Figure **2** transmission electron micrographs of smoke particles from flaming acetylene and ethylene can be seen [9]. These are chain like structures, called agglomerates as they are made up of an agglomeration of small primary particles, typically **20** nm to **80** nm in diameter depending on fuel and combustion conditions. It is also apparent from the TEM images, which have the same magnification, that the primary spheres for the acetylene smoke are larger (about **30** %) than the ethylene primary spheres. The size distribution of the acetylene agglomerates ranged from about **0.04** μm to **20** μm [9].

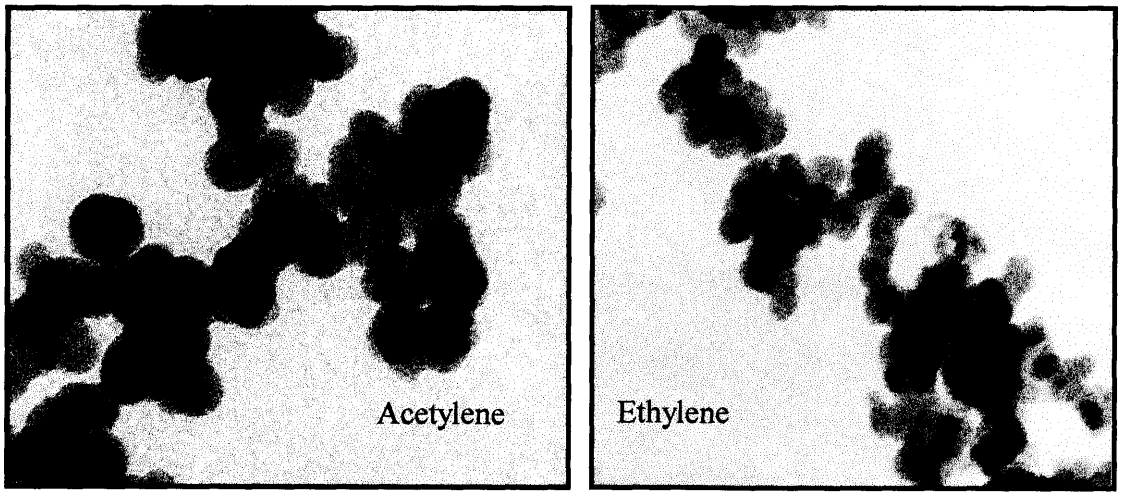

Figure 2: Transmission Electron Microscope image of acetylene and ethylene used by Mulholland and Choi [9], both images are at the same magnification, 50,000x.

4. Light Scattering Measurements

The light scattering properties of the smoke particles were examined using the LAOF's

differential scattering system and methodology described elsewhere [8]. The differential (angular distribution) scattering study presented here has examined the scattering of linearly polarized light for the scattering angles between 5° and 135°, and determined the

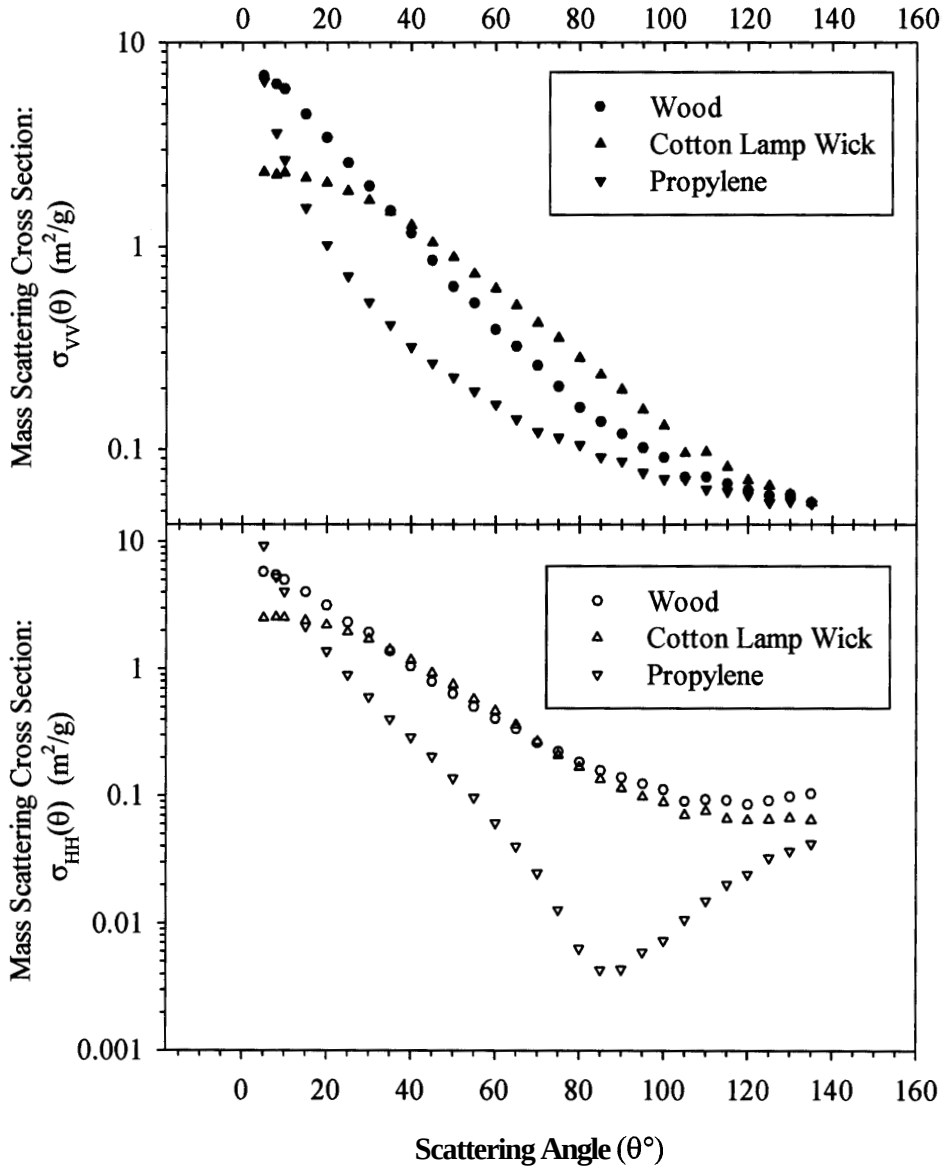

Figure 3: Differential mass scattering cross section for wood, cotton lamp wick and propylene smoke particles generated in the Fire Emulator/ Detector Evaluator at NIST

smoke particle's differential mass scattering cross sections, $\sigma_{VV}(\theta)$ and $\sigma_{HH}(\theta)$, for different polarizations. The first subscript denotes the incident polarization and the second denotes scattered polarization measured: V for vertical and H for horizontal to the scattering plane. The differential mass scattering cross section is determined in units of area (m^2) per particle mass (g) at a given scattering angle, θ. Figure 3 shows the differential **mass** scattering cross section for the three smokes produced in the FE/DE at MST. The fractional combined uncertainty (based on one standard deviation) of the differential **mass** scattering cross sections varies but is typically in the range of **10 %** to **20** % due mainly to the calibration with monosize polystyrene spheres [8]. The effect of larger mean size of the wood smoke particles on the scattering cross section, $\sigma_{VV}(\theta)$, can be seen in the steeper slope in the forward direction as opposed to the less steep slope for the cotton wick results. The comparison of the two non-flaming fuel smokes for HH polarization shows that their values are similar at most angles except the forward angles and near 135°. The smooth curves for the non-flaming fuel smoke particles seen in Figure **3** are a result of the polydisperse nature of these smoke aerosols. Scattering from polydisperes ensembles of particles averages out the detail seen in single particle scattering data.

5. Treatment of Polarization

The information in Figure 3 can be rearranged to give the degree of linear polarization, $P(8)$, (with angular notation suppressed)

$$P = \frac{\sigma_{VV} - \sigma_{HH}}{\sigma_{HH} + \sigma_{VV}} \tag{1}$$

The quantity $P(\theta)$ has previously been measured for the **EN54** test smokes over an angular range of **5** to **165° [6].** The degree of polarization for the FE/DE generated smokes is shown in Figure 4, along with the theoretical curve expected from Rayleigh scattering. The deviation from $P(0) = 0$ in Figure 4 is due to polarization dependent errors in the optical system, particularly for the propylene. The other results are mainly influenced by the uncertainty in the calibration **[8].** The results in Figure **4** compare well with **[6]** as they found the highest degree of polarization corresponded to the soot particles, a medium value existed for the cotton wick smoke, and that the lowest values

were found for the pyrolyzed wood smoke.

Another widely used and related measure is the polarization ratio, defined as

$$\rho(\theta) = \frac{\sigma_{HH}(\theta)}{\sigma_{VV}(\theta)} \tag{2}$$

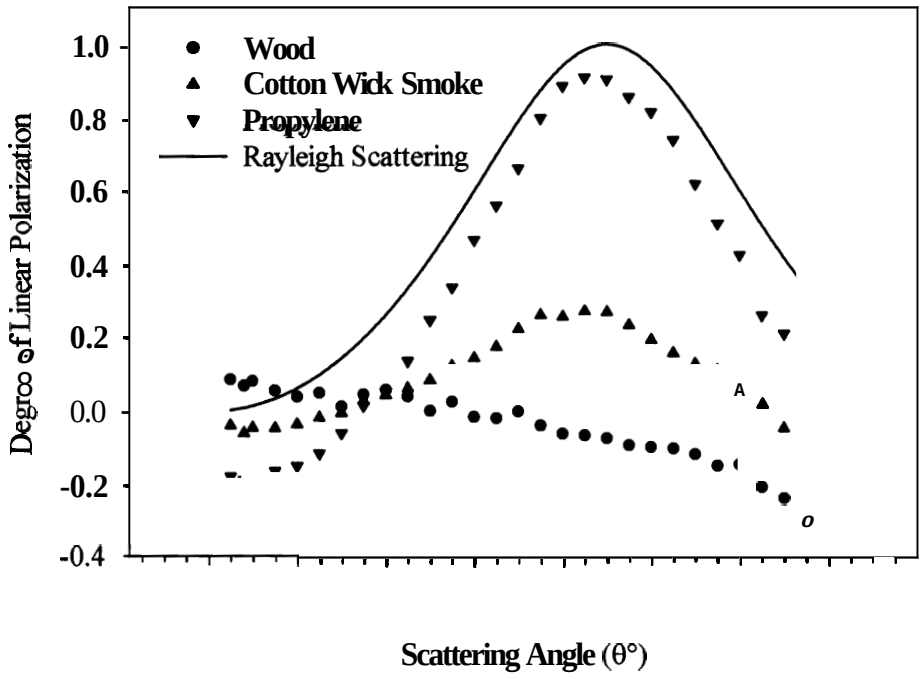

Figure 4: Degree of linear polarization, $P(\theta)$, for the FEDE produced smoke particles.

Table 1 includes the polarization ratio at 90° for the FEDE smokes and two other soots, acetylene and ethylene, generated using a laminar co-flow diffusion burner [8]. The degree of polarization or the polarization ratio in Table 1 indicates that two detectors positioned perpendicular to each other, with incident linear polarized light, could distinguish between smoke from flaming or non-flaming fires. The greatest difference in $P(8)$ or $\rho(\theta)$ for the flame generated smoke versus non-flaming occurs at $8 = 90°$. The ratio of polarization is also sensitive to the fuel for flame generated smoke particles

(see Table 1), which is related to the soot agglomerates different primary particle diameters. Previous measurements [9] indicate that the primary shpere size is affected by the fuel type, and this may account for the fuel dependence of $\rho(\theta)$.

6 Fractal Analysis of Scattered Light

It has been stated that the high values of the degree of polarization (i.e. near $\theta = 90°$, $P(\theta) \rightarrow 1$) for flame generated smokes is due to their particle size being small compared to the wavelength of the incident beam [6]. This is misleading in that it implies the soot particles scatter light according to Rayleigh theory. The scattering from agglomerates with sizes up to 20 μm [9] is more complex than Rayleigh theory.

The total scattering from a soot agglomerate can be represented as (angular notation suppressed)

$$\sigma_{XX} = \left(S_{ag} \cdot S_r\right)_{XX} \quad \text{but} \quad \left(S_{ag}\right)_{VV} \approx \left(S_{ag}\right)_{HH} \tag{3}$$

where S_r is the Rayleigh-like scattering component and **X** denotes a given polarization. The term S_{ag} arises from the interference in the far field of the Rayleigh scattering by the individual primary particles making up the agglomerate. The term, S_{ag}, can vary by three orders of magnitude (Figure 3) while for Rayleigh scattering, $(S_r)_{VV}$,is

Fuel	Degree of Polarization	Polarization Ratio
	P (90/120)	P (90/120)*	$\rho(90°)$
Wood (flaming)	--	0.94 / 0.5	--
Wood (pyrolysed)	-0.07 / -0.15	-0.12 / -0.25	1.16
Cotton wick	0.27 / 0.05	0.3 / 0.13	0.58
Propylene	0.90 / 0.43	--	0.05
Acetylene	0.96 / 0.53	--	0.023
Ethylene	0.97 / 0.51	--	0.013

Table 1: Ratio of linear polarization at $\theta = 90°$, for various smoke particles: wood, cotton wick and propylene generated in the FE/DE ; while acetylene and ethylene were generated in a co-flow laminar diffusion burner [10]. * data has been taken from [6].

independent of angle. Since S_{ag} is independent of the polarization direction it is effectively reduced in the polarization ratio, $\rho(6)$, which then reflects the Rayleigh-like scattering from the primary spheres.

The general formalism of agglomerate light scattering [11] can be expressed in terms of the scattering parameter q which follows a power law relation that reduces to $\sigma_{VV}(6) \propto q^{-D}$ for $q > R^{-1}$: where R is the agglomerate characteristic radius; $q = 4\pi\lambda^{-1}\sin(\theta/2)$ is the elastic scattering wavevector magnitude or scattering parameter; and D is the fractal dimension characterizing the agglomerate. Various studies for in-flame and post-flame soot have reported fractal dimensions to be about **1.7** to **1.85** using laser scattering techniques [12]. This general behavior is related to the fact that all soot shares the same fundamental mechanisms of agglomeration growth [13].

Fuel	Fractal Dimension, D	
Acetylene	**1.6**	1.85*
Ethylene	**1.7**	1.84*
polypropylene	**1.8**	**1.83***

Table 2: Fractal dimensions determined from Figure **5**, for $q \geq 5.1\ \mu m^{-1}$ and (*) results reported by [14].

Figure **5** shows the log-log plot for mass scattering cross section (vertical-vertical polarization) as a function of the scattering parameter, q, for the three soots, ethylene, acetylene and propylene, as well as the smoke from wood and cotton wick. The slopes for the soots at $q \geq 5.1\ \mu m^{-1}$ are tabulated in Table **2** and compared with another study [14]. The low value for acetylene might be due to the presence of super-agglomerates ($>> 50\ \mu m$).

We also observe in Figure **5** that there is a qualitative difference between the q dependence for soot compared to non-flaming smoke particles. The higher forward scattering for the wood smoke is apparent and the slope for scattering angles

corresponding to $q \geq 12\ \mu m^{-1}$ ($\theta \geq 75°$) yield slopes of about 3 and 4.6 for wood and cotton wick smoke respectively. The exact relationship in the context of Mie theory between these qualitative differences and the morphology, size and refractive index of a scattering particle is only recently being considered [10]. A detector with a diode array in the back scattering angles could be used to compare the slope of the signal when treated as a function of q. Large integer values of the slope, ≥ 3, would indicate compact scattering particles while small values, ≤ 2, would indicate open agglomerates. There is a need to obtain data for a wide range of non-flaming smokes as well as nuisance aerosol results to assess the utility of this approach.

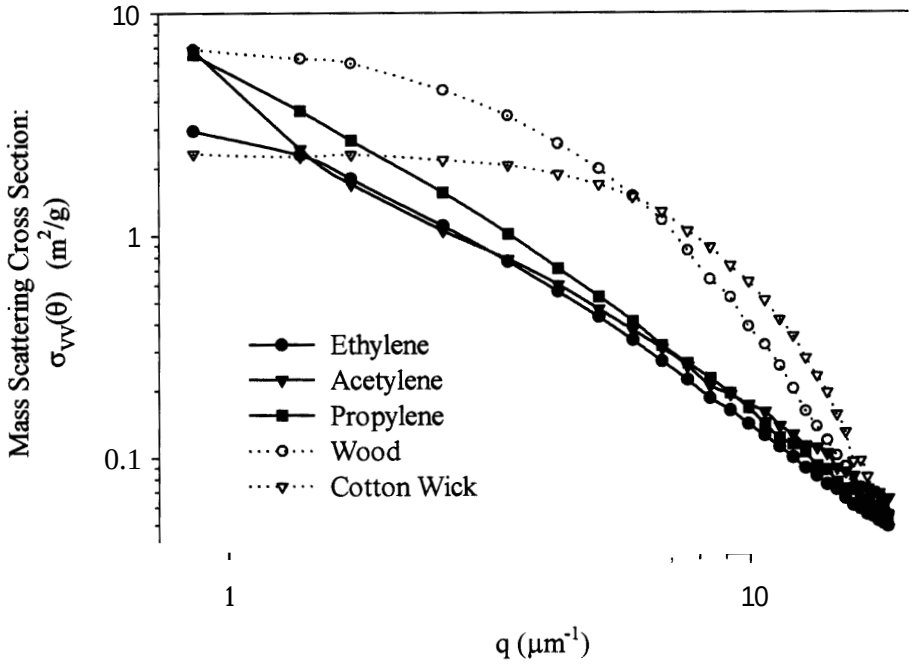

Figure 5: Mass scattering cross section (VV) as plotted against the scattering wavevector, q.

6 Conclusion

This study presents results for the first time of the mass scattering cross section ($m^2\ g^{-1}$) of smokes similar to those used in smoke detector standards EN54 and UL 217. Smokes

were generated in the fire emulator/detector evaluator (FEDE) at NIST and characterized in terms of their size and optical properties. The size characterization shows that the smoke from pyrolysed wood blocks is a unimodal distribution with a MMAD of **1.6** μm, while the smoldered cotton lamp wick fuel has a bimodal distribution with a MMAD of **0.3** μm for its measurable mode. It was found that **48 %** of the mass of the cotton wick smoke was below **0.056** pm. The difference in mass/aerodynamic diameter is also observed in the differential **mass** scattering cross sections for near forward scattering angles, where the wood smoke scatters light more strongly than cotton wick smoke particles due to its larger mean size.

The ratio of polarization and the degree of linear polarization have been demonstrated **as** a means of distinguishing between soot from flaming fires and smoke particles from non-flaming fires. The ratio of polarization is shown to be more sensitive than the degree of polarization to soots from different flaming fuels, probably due to the different primary particle size. All three flame generated smokes are shown to have similar "q" plots, which are easily distinguished from the two "q" plots for the non-flaming fuels smokes.

Reference List

[1] Grosshandler WL: Towards the development of a universal fire emulator-detector evaluator. ***Fire Safety Journal*** **1997; 29:113-127**

[2] Cleary, T., Donnelly, M., and Grosshandler, **W.** The Fire Emulator/Detector Evaluator: Design, Operation and Performance. 12th International Conference on Automatic Fire Detection. Grosshandler, **W.**

[3] Helsper **C,** Fissan HJ, Muggli J, Scheidweiler A: Particle number distributions of aerosols from test fires. ***Journal of Aerosol Science*** **1980;** 11**:439-446**

[4] Tamm E, Mirme A, Sievert U, Franken D: Aerosol particle concentration and size distribution measurements of test-fires **as** a background for fire detector modelling. ***Internationale Konferenz uber Automatische Brandentedekung, AUBE '99*** **1999;150-159**

[5] Meacham **BJ,** Motevalli V: Characterization of smoke from smoldering

combustion for the evaluation of light scattering type smoke detector response. ***Journal of Fire Protection Engineering*** **1992; 4:17-28**

[6] Loepfe M, Ryser P, Tomkin C, Wieser D: Optical properties of fires and non-fire aerosols. ***Fire Safety Journal*** **1997; 29:185-194**

[7] Marple VA, Rubow KL, Behm SM: A Microorifice Uniform Deposit Impactor (MOUDI): Description, calibration and use. ***Aerosol Science and Technology*** **1991;** 14:434-446

[8] Weinert, D. and Mulholland, G. W. An apparatus for light scattering studies of smoke particles. 12th International Conference of Automatic Fire Detection AUBE, **2001.**

[9] Mulholland, G. **W.** and Choi, M. **Y.** Measurement of the mass specific extinction coefficient for acetylene and ethylene smoke using the large agglomerate optics facility. The Combustion Institute. Twenty-Seventh Symposium (international) on Combustion. **1515-1522.98.** Pittsburgh, The Combustion Institute.

[10] Sorensen CM, Fischbach DJ: Patterns in Mie Scattering. ***Optics Communications*** **2000;** 173:145-153

[11] Sorensen CM: Light Scattering from Fractal Aggregates. ***To be submitted for publication***

[12] Sorensen CM, Feke GD: The morphology of macroscopic soot. ***Aerosol Science and Technology*** **1996;** 25:328-337

[13] Mountain RD, Mulholland GW: Light scattering from simulated smoke agglomerated. ***Langmuir*** **1988; 4:1321-1326**

[14] Koylu UO, Faeth GM, Farias TL, Carvalho MG: Fractal and projected structure properties of soot agglomerates. ***Combustion and Flame*** **1995;** 100:621-633